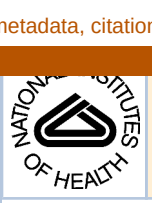



Published in final edited form as:
*Pharmacogenet Genomics*. 2007 February ; 17(2): 145–160.

# Identification and functional characterization of polymorphisms in human cyclooxygenase-1 (*PTGS1*)

**Craig R. Lee**[a,b], **Frank G. Bottone Jr**[a], **Joseph M. Krahn**[a], **Leping Li**[a], **Harvey W. Mohrenweiser**[c,d], **Molly E. Cook**[a], **Robert M. Petrovich**[a], **Douglas A. Bell**[a], **Thomas E. Eling**[a], and **Darryl C. Zeldin**[a]

a*Division of Intramural Research, National Institute of Environmental Health Sciences, National Institutes of Health, Research Triangle Park*

b*Division of Pharmacotherapy and Experimental Therapeutics, School of Pharmacy, University of North Carolina at Chapel Hill, Chapel Hill, North Carolina*

c*Biology and Biotechnology Research Program, Lawrence Livermore National Laboratory, Livermore, California*

d*Center for Research in Occupational Toxicology, Oregon Health and Sciences University, Portland, Oregon, USA*

## Abstract

**Objective—**Cyclooxygenase-1 (COX-1, *PTGS1*) catalyzes the conversion of arachidonic acid to prostaglandin $H_2$, which is subsequently metabolized to various biologically active prostaglandins. We sought to identify and characterize the functional relevance of genetic polymorphisms in *PTGS1*.

**Methods—**Sequence variations in human *PTGS1* were identified by resequencing 92 healthy individuals (24 African, 24 Asian, 24 European/Caucasian, and 20 anonymous). Using site-directed mutagenesis and a baculovirus/insect cell expression system, recombinant wild-type COX-1 and the R8W, P17L, R53H, R78W, K185T, G230S, L237M, and V481I variant proteins were expressed. COX-1 metabolic activity was evaluated *in vitro* using an oxygen consumption assay under basal conditions and in the presence of indomethacin.

**Results—**Forty-five variants were identified, including seven nonsynonymous polymorphisms encoding amino acid substitutions in the COX-1 protein. The R53H (35 ± 5%), R78W (36 ± 4%), K185T (59 ± 6%), G230S (57 ± 4%), and L237M (51 ± 3%) variant proteins had significantly lower metabolic activity relative to wild-type (100 ± 7%), while no significant differences were observed with the R8W (104 ± 10%), P17L (113 ± 7%), and V481I (121 ± 10%) variants. Inhibition studies with indomethacin demonstrated that the P17L and G230S variants had significantly lower $IC_{50}$ values compared to wild-type, suggesting these variants significantly increase COX-1 sensitivity to indomethacin inhibition. Consistent with the metabolic activity data, protein modeling suggested the G230S variant may disrupt the active conformation of COX-1.

**Conclusions—**Our findings demonstrate that several genetic variants in human COX-1 significantly alter basal COX-1-mediated arachidonic acid metabolism and indomethacin-mediated inhibition of COX-1 activity *in vitro*. Future studies characterizing the functional impact of these variants *in vivo* are warranted.

Correspondence and requests for reprints to Dr Darryl C. Zeldin, MD, National Institute of Environmental Health Sciences, 111 T.W. Alexander Drive, Research Triangle Park, NC 27709, USA Tel: + 1 919 541 1169; fax: + 1 919 541 4133; e-mail: zeldin@niehs.nih.gov

**Keywords**

COX-1; cyclooxygenase-1; polymorphism; *PTGS1*

## Introduction

Cyclooxygenases (COX)-1 and COX-2 catalyze the oxidative conversion of arachidonic acid to prostaglandin (PG) $H_2$, which is subsequently metabolized to various biologically active metabolites such as prostacyclin and thromboxane $A_2$ [1]. Although both COX-1 and COX-2 catalyze the same metabolic reaction with similar efficiencies, they are encoded by distinct gene products and differ substantially in their regulation and expression [1].

The gene encoding human COX-1 (*PTGS1*) has been mapped to chromosome 9q32–q33.3, is approximately 22 kb in length, and contains 11 exons [2,3]. COX-1 is constitutively expressed and is responsible for the biosynthesis of PGs involved in various housekeeping functions, such as the regulation of renal, gastrointestinal, and platelet function [1]. COX-2 (*PTGS2*) is induced by multiple biological mediators, and primarily catalyzes PG synthesis in cells involved in both local and systemic inflammatory responses [1]. Nonsteroidal anti-inflammatory drugs (NSAIDs) inhibit COX-mediated PG synthesis and are widely used for the prevention and/or treatment of various diseases [4]. As a therapeutic class, these agents demonstrate a wide range of relative selectivity for COX-1 and COX-2, and significant interindividual variability in clinical response exists [4]. Owing to the inducible nature of COX-2 regulation and its potential role in the pathogenesis of various inflammatory disorders, the overwhelming majority of research characterizing the role of COXs in human disease to date has focused on COX-2. Recent evidence, however, including associations between selective COX-2 inhibitor utilization and myocardial infarction risk, suggests the relative contribution of COX-1 and COX-2-mediated PG synthesis is important [5,6]. Consequently, genetic variation in both *PTGS1* and *PTGS2* may be important modifiers of disease risk in humans.

The identification and functional characterization of genetic polymorphisms in *PTGS2* have been reported [7,8]. These studies demonstrate that certain variants significantly alter COX-2 expression and/or activity, and may be important risk factors for disease in humans [7-9]. In contrast, characterization of genetic variation in *PTGS1* has not been as widely investigated, even though the presence of functionally relevant variants may significantly influence PG biosynthesis, disease risk, and NSAID pharmacodynamics in humans. Polymorphisms in both coding and noncoding regions of human *PTGS1* have been previously identified [10-13], and *PTGS1* has been resequenced as part of the Seattle SNPs Variation Discovery Resource (http://pga.mbt.washington.edu/). In particular, nonsynonymous variants encoding amino-acid substitutions in the COX-1 protein have been identified [10-13]. The functional consequences of these variants, in terms of their influence on basal COX-1-mediated arachidonic acid metabolism, however, have not been characterized to date. Human studies have evaluated the potential influence of certain variants on NSAID-mediated inhibition of COX metabolism *in vivo* and *ex vivo* [12,14-16]; however, the functional consequences of most variants on NSAID pharmacodynamics are not well understood. Our primary objectives were to: (i) identify or confirm the existence of polymorphisms in *PTGS1* by resequencing, (ii) characterize the linkage disequilibrium (LD) structure in *PTGS1*, and (iii) evaluate the functional consequences of selected variants using established in-vitro assays.

# Methods

## Chemicals

All chemicals were purchased from Sigma (St Louis, Missouri, USA), unless otherwise noted.

## DNA samples

Genomic DNA was extracted from 72 human lymphoblastoid cell lines (Coriell Institute, Camden, New Jersey, USA) obtained from healthy individuals with the following ancestries: 24 Africans (16 African-Americans, eight African Pygmy), 24 Asians (five Indo-Pakistani, five native Taiwanese, five mainland Chinese, three Cambodian, three Japanese, three Melanesian), 24 European/Caucasians (nine European-Americans, five Druze, five Adygei, five Russian), and an additional 20 anonymous healthy US residents (DNA Polymorphism Discovery Resource, NIH) [17], as part of the NIEHS Environmental Genome Single Nucleotide Polymorphism (egSNP) program (http://dir-apps.niehs.nih.gov/egsnp/home.htm) [7,18-20].

## Genotyping

A resequencing strategy was used to identify variants in both coding and noncoding regions of *PTGS1*. Sequencing spanned all 11 exons, including approximately 75 bp 3′ and 5′ of each intron–exon boundary, and 2.4 kb into the 5′-untranslated region (5′UTR). Amplified polymerase chain reaction products containing these regions were generated using oligonucleotide primers specific to *PTGS1* (Table 1). All sequencing was performed in both directions as previously described [7,18-20]. As all DNA samples came from commercially available cell lines, this protocol was considered exempt by the Lawrence Livermore National Laboratory Institutional Review Board.

## Linkage disequilibrium statistics

Minor allele frequencies and pairwise LD statistics were calculated for each polymorphism, and the corresponding LD plots were generated (Haploview 3.2, Broad Institute of Harvard and MIT, Cambridge, Massachusetts, USA) [21]. All analyses were completed independently in the African, Asian, and European/Caucasian ethnic groups.

## Evaluation of COX-1 gene and protein sequences

We extracted approximately 1.8 kb of the human *PTGS1* 5′UTR sequence from the University of California Santa Cruz Genome Browser (http://genome.ucsc.edu/), and aligned the corresponding human, mouse, rat, dog, and chimp sequences for this region to screen for nucleotide conservation across species at each of the polymorphic sites. We then evaluated the sequences surrounding each polymorphism for potential location within putative transcription factor binding sites using the TRANSFAC database [22].

The human, rat, mouse, and sheep COX-1 amino-acid sequences were obtained from Genbank (U.S. National Library of Medicine, Bethesda, Maryland, USA) and aligned using the ClustalW program [23] to determine whether the identified nonsynonymous polymorphisms occurred in conserved regions of the protein. A model of the human COX-1 protein was constructed based on the ovine COX-1 crystal structure (PDB accession 1Q4G) [24], which has 96% sequence identity to human COX-1. The model was also compared with the murine COX-2 crystal structure (PDB accession 1CVU) [25,26]. Additional crystallographic refinement was performed for both structures using the deposited diffraction data after analysis by MolProbity (Duke University, Durham, North Carolina, USA) [27]. In both cases, the crystallographic R-factor was reduced by more than 1% in working and test reflection sets. The procedure for modeling human COX-1 from the refined ovine structure consisted primarily of selecting

preferred rotamers [27]. The high level of sequence conservation and lack of insertions or deletions eliminated the need for changes to the C-α backbone coordinates. Substitution of side chains using common side-chain rotamers produced an acceptable fit in all cases, so no energy minimization was performed. To predict the potential impact of amino-acid substitutions on the structure and function of the COX-1 protein, the R53H, R78W, K185T, G230S, L237M, and V481I variant amino acids were individually built into the wild-type (WT) human COX-1 model. As the R8W and P17L polymorphisms occur in the COX-1 signal peptide and the ovine COX-1 crystal structure starts at amino-acid residue 25 [24], the impact of these variants was not evaluated in the model.

### Plasmid construction and site-directed mutagenesis

The full-length COX-1 cDNA was subcloned into pcDNA3.1 (Invitrogen, Carlsbad, California, USA), as previously described [28]. Single nucleotide polymorphisms (SNPs) were introduced into the WT COX-1 cDNA by site-directed mutagenesis using the QuikChange Site-Directed Mutagenesis Kit (Stratagene, La Jolla, California, USA) as per the manufacturer's instructions. The specific primer sequences used to generate each of the eight mutations are provided in Table 2. Presence of the desired mutation in each ampicillin-resistant clone was confirmed by sequencing the entire COX-1 cDNA using the BigDye Terminator Reaction Ready Mix (Applied Biosystems, Foster City, California, USA) and ABI Prism 377 DNA sequencer (Applied Biosystems). WTand variant cDNAs with the desired substitutions and no secondary mutations were then subcloned into the *Bam*HI/*Not*I sites of the pVL1393 Baculovirus Transfer Vector (BD Biosciences, San Diego, California, USA) via the intermediate pCR Blunt II-TOPO vector (Invitrogen). The orientation and sequence of the WT and variant cDNAs in pVL1393 were confirmed by direct sequencing.

### Expression of human COX-1 in Sf9 cells

Sf9 cells were plated in T-25 tissue culture flasks at $2 \times 10^6$ cells/flask, cotransfected with 0.5 μg of BaculoGold Bright linearized baculovirus DNA (BD Biosciences) and 2 μg of pVL1393 containing the COX-1 inserts, and incubated at 271C for 96 h. Recombinant baculovirus was amplified by infecting 50 ml of Sf9 cells (70% confluent) in HyQ SFX-Insect cell culture media (Fisher Chemical, Fairlawn, New Jersey, USA) and 5% fetal bovine serum with 1 ml of the transfection supernatant, and incubated in spinner flasks for 72 h at 27°C at 120 r.p.m. Cells were harvested and lysed by sonication in 80 mmol/l Tris, 2 mmol/l ethylenediaminetetraacetic acid (EDTA) buffer (pH = 7.2). Viral amplification was qualitatively confirmed by visualizing green fluorescent protein fluorescence in the lysed cells under ultraviolet light. Uninfected negative control cells demonstrated no fluorescence. For large-scale COX-1 expression, 1000 ml of Sf9 cells (70% confluent) were infected with each amplification supernatant and incubated for 72 h in spinner flasks at 27°C at 120 r.p.m., as described [7,29,30]. Cells were centrifuged for 20 min at 4°C at 3000 r.p.m., washed with ice-cold phosphate-buffered saline, and centrifuged again. Cell pellets were stored at −80°C after removal of the supernatant.

Cell pellets were thawed on ice and lysed by sonication in an 80 mmol/l Tris, 2 mmol/l EDTA buffer (pH = 7.2) containing 0.1 mol/l silver diethyldithiocarbamate and protease inhibitors, as described [7,29,30]. Cell lysates were ultracentrifuged at 40 000 r.p.m. at 4°C for 1 h, and the microsomal pellets were homogenized in a 200 mmol/l Tris, 0.1 mmol/l EDTA buffer (pH = 8.0) containing 0.4% CHAPS. Homogenates were stirred for 1.5 h at 4°C while bringing the final volume to 1% CHAPS (w/v), and ultracentrifuged at 40 000 r.p.m. at 4°C for 45 min. Supernatants, which contained the solubilized COX-1 enzyme, were stored in aliquots at −80° C.

### Immunoblotting

Protein concentrations of the solubilized microsomal fractions were quantified using the Bio-Rad protein assay (Bio-Rad, Hercules, California, USA). Protein normalized samples were added to 4× sample buffer containing β-mercaptoethanol and boiled for 5 min. Proteins were separated by 10% Novex Tris-glycine polyacrylamide gels (Invitrogen) and transferred to nitrocellulose membranes (Invitrogen) in transfer buffer containing 20% methanol. The membranes were blocked in 5% nonfat milk in Tris-buffered saline for 2 h, incubated in a 1 : 250 dilution of COX-1-specific monoclonal antibody (Cayman Chemical, Ann Arbor, Michigan, USA) at 4°C overnight, and then washed in 0.05% Tris-buffered saline-Tween-20 four times. After incubation with a 1 : 2000 dilution of horseradish peroxidase-conjugated bovine antimouse secondary antibody (Santa Cruz Biotechnology, Santa Cruz, California, USA) and additional washing, COX-1 immunoreactive bands were detected by chemiluminescence using the SuperSignal West Pico chemiluminescent substrate (Pierce, Rockford, Illinois, USA).

To estimate differences in COX-1 expression across each preparation, densitometry was completed after multiple immunoblots and mean fold differences in COX-1 immunoreactivity were calculated for each variant relative to WT. The total amount of solubilized microsomal protein used in all subsequent activity studies was normalized to COX-1 immunoreactivity based on these calculations. Similar protein normalization methods have been utilized for the functional characterization of nonsynonymous polymorphisms in other genes using a baculovirus/insect cell expression system [7,19].

### COX-1 enzymatic assay

COX-1 enzymatic activity was determined by measuring oxygen consumption at 37°C in an oxygraph chamber using an YSI Model 53 oxygen monitor and electrode (YSI International, Yellow Springs, Ohio, USA), as described [7,29-31]. The reaction buffer consisted of 100 mmol/l Tris (pH = 8.0) containing 500 μmol/l phenol. Solubilized microsomal protein from the WT (3.4 mg of total protein) and eight variant (total protein amounts normalized to COX-1 immunoreactivity) preparations were reconstituted in reaction buffer with 10 μmol/l hematin for 1 min on ice. Solubilized microsomal protein from uninfected Sf9 cells (3.4 mg of total protein) was used as a negative control. Samples were then equilibrated in reaction buffer for 1 min at 37°C. Oxygen consumption was measured for 120 s following the addition of 100 μmol/l arachidonic acid (Cayman Chemical), and the rate of oxygen consumption was calculated and expressed as μmol/l$O_2$/min/mg microsomal protein. Three independent experiments were completed, each in triplicate.

Inhibitor studies were completed with 0 (vehicle), 0.1, 1, 5, 10, and 25 μmol/l indomethacin (Cayman Chemical) in the WT, R8W, P17L, G230S, and L237M preparations. Solubilized microsomal proteins were reconstituted on ice for 10 min with hematin plus indomethacin, each completed in triplicate, and oxygen consumption was measured using the experimental conditions described above.

### Statistical analysis

The rate of oxygen consumption was expressed relative to WT and averaged. Data are presented as mean ± standard error of the mean, and were compared across COX-1 preparation by analysis of variance. A post-hoc Dunnett's test assessed the presence of statistical differences between each mutant relative to WT. A *P*-value of $<0.05$ was considered statistically significant.

To determine whether certain variants significantly influenced indomethacin-mediated inhibition of COX-1, $IC_{50}$ values were estimated. First, the data for each preparation were plotted as percent activity relative to control (vehicle) versus natural log indomethacin

concentration. The $IC_{50}$ value for each was estimated according to the Hill equation by nonlinear regression (WinNonlin, Pharsight Corporation, Mountain View, California, USA), where $E_{max} = 1.0$, $C$ = natural log indomethacin concentration, and the $IC_{50}$ and γ (an exponential term influencing the sigmoidal shape of the curve) values were estimated according to the model's fit of the data:

$$\text{Effect} = E_{max} \times \left[1 - \left(\frac{C_{\gamma}}{C_{\gamma} + IC_{50\gamma}}\right)\right].$$

Triplicate values at each indomethacin concentration were simultaneously modeled for estimation of a single $IC_{50}$ value ( ± 95% confidence intervals) for each preparation. Inclusion of a $1/Y^2$ weighting factor substantially improved the model's fit of the data according to the Akaike information criterion value.

## Results

### Identification of *PTGS1* variants

Sequencing the *PTGS1* gene in 72 individuals of known ethnicity identified 44 variants (42 SNPs, one nucleotide insertion, and one nucleotide deletion). Evaluation of an additional 20 anonymous individuals of unknown ethnicity identified one additional SNP. Of these 45 variants, 14 were located in the 5′UTR, 12 were in exons, and 19 were in introns. Seven of the 12 exonic substitutions were nonsynonymous (R8W, R8P, P17L, R78W, K185T, L237M, and V481I) and five were synonymous. The R8P and R78W variants have not been previously reported. The R8P variant was identified in a single individual of African descent. The R78W variant was identified in a single individual of unknown ethnicity. The R53H and G230S variants reported in other populations [10,12] were not identified in this resequencing analysis; however, we confirmed their existence at frequencies <1% in an independent African-American population ($n = 367$) (data not shown). The minor allele frequencies of most polymorphisms differed significantly across ethnicity, with the Asian sample demonstrating the least genetic variation. The location minor allele frequencies, and other details for all 45 variants are summarized in Table 3. Given the magnitude of genetic diversity and admixture across human populations, and the small number of chromosomes screened within each ethnic group, the reported minor allele frequencies should be considered an approximation.

### Linkage disequilibrium structure of the *PTGS1* gene

The LD structure across *PTGS1* is presented for each ethnicity (Fig. 1). A substantial degree of LD was observed throughout the 5′UTR. This LD pattern specifically involved seven polymorphisms (*T-1749C*, *G-1598A*, *A-1202G*, *A-1201G*, *G-1006A*, *A-918G*, and *A-707G*) (Table 3) and was observed in both the European/Caucasian ($D' = 1.0$, $r^2 = 0.73–1.0$) and African ($D' = 1.0$, $r^2 = 1.0$) samples, suggesting that these seven polymorphisms are on the same haplotype. In European/ Caucasians, these 5′UTR polymorphisms were also in significant LD with the P17L variant in exon 2. Interestingly, only two of the identified 5′UTR polymorphisms (*C-1160G* and *G-951A*) are located in regions relatively conserved across human, mouse, rat, dog, and chimp, suggesting that most are in regions that are not selectively constrained. Our transcription factor binding site search suggests that the *T-1749C* polymorphism could weaken a putative AML/RUNX1-binding site by changing the core motif from *TGTTGT* to *TGCTGT*, the linked *A-1202G* and *A-1201G* polymorphisms could destroy a putative NF-Y-binding site by changing the core NF-Y motif from *CCAAT* to *CCGGT*, and the *G-951A* polymorphism could disrupt a putative NF-AT-binding site. In addition, the *G-1006A* polymorphism could create a putative heat shock protein-binding site.

## Structural analysis of the COX-1 protein

Alignment of human, mouse, rat, and sheep COX-1 amino-acid sequences demonstrated that the R78, G230, and L237 amino acids are conserved across each of these species (Fig. 2). Interestingly, L237 is also conserved across all COX-2 protein sequences. The R53H, R78W, K185T, G230S, L237M, and V481I variants were individually incorporated into the WT human COX-1 model (Fig. 3). Substitution of a serine for glycine at residue 230 (G230S) appears to significantly impact the structure of COX-1 (Fig. 4). First, glycine 230 is located on a $3_{10}$ helical turn, suggesting that this tight turn requires a glycine residue. The equivalent residue in COX-2 is asparagine 231. Comparison of our model to murine COX-2 (PDB accession 1CVU) [25,26] reveals that some of the backbone interactions in COX-2 are less favorable than observed in COX-1, but these are offset through favorable interactions by the asparagine 231 side chain to the backbone carbonyl of glutamine 208 and the side chain of aspartic acid 229 (Fig. 4c). In our human COX-1 model, there is a single sterically compatible rotamer conformation for serine 230 substitution, which can interact favorably with only one hydrogen-bond acceptor (Fig. 4b). The minimum conformational change to avoid a negative interaction is the rotation of aspartic acid 228 to a position within hydrogen-bonding distance to arginine 332. This position, however, requires a displacement of tryptophan 138′, which perturbs the dimer interface association, potentially influencing enzyme activity (Fig. 4d, where ‘prime’ indicates a residue from the dimer associated molecule). Moreover, arginine 332 is solvent-accessible at the bottom of a narrow crevasse where arachidonic acid could form hydrogen bonds and prevent stabilization of the proposed alternate conformation of aspartic acid 228.

In the presence of the R53H, R78W, K185T, L237M, or V481I substitutions, common rotamer conformations yielded reasonable accommodation of the substituted amino acid; however, in certain cases potential minor alterations in structure that could influence enzyme activity were noted. For instance, arginine 53 is in a solvent exposed region where substitution with histidine (R53H) has no obvious effects; however, this substitution could have a minor influence on glycosylation of asparagine 67 or the adjacent dimerization contact, both of which are approximately about 10–11 Å away. The arginine 78 residue is at the membrane binding surface, and, although conserved, a tryptophan substitution at this position (R78W) is also favorable for membrane binding and unlikely to directly influence enzyme activity. The most feasible functional role for arginine at this site would be to assist retrieval of arachidonic acid into the active site. The lysine 185 residue is on a solvent exposed loop, distant from any functional site likely to influence catalysis; however, this residue is in a positively charged region with several arginines, which could serve some nonobvious function potentially altered by a threonine substitution (K185T). The leucine 237 residue is likely involved in a dimerization interaction, with significant contacts to sugars linked to asparagine 143 of the related monomer. A methionine substitution (L237M) fits reasonably well into this site with favorable hydrophobic interactions, but it is larger and more flexible. This mutation is predicted to have a small effect on the dimerization interface. Moreover, oxidation of methionine could conceivably impact the dimerization contact; however, it is unclear whether either of these effects could significantly influence enzyme activity. The valine 481 residue is distant from both the catalytic site and dimerization surface. As an isoleucine substitution (V481I) is conservative, this mutation appears unlikely to influence enzyme activity.

## Expression of the wild-type and variant COX-1 proteins

The COX-1 WT and mutant R8W, P17L, R53H, R78W, K185T, G230S, L237M, and V481I proteins were expressed in Sf9 cells using a single promoter baculovirus system. The R8P variant was not expressed as the R8W variant occurred at the same amino-acid position and was more frequent. Expression was verified by immunoblotting, with a molecular mass of approximately 70 kDa for the WT and mutant proteins (Fig. 5a). COX-1 expression was not

observed in uninfected Sf9 cells. Consistent with previous studies of COX-1 expression in Sf9 cells [29,30], the relative amount of COX-1 in the solubilized microsomal fraction to the total amount of protein was fairly low. Large-scale expression of each preparation, however, generated enough COX-1 protein for functional characterization.

Densitometry analysis of multiple immunoblots demonstrated variability in the level of COX-1 immunoreactivity across preparations, with an approximate range of 0.3–1.4-fold difference relative to WT. Immunoblots were repeated with varying amounts of solubilized microsomal protein according to these densitometry results to normalize each preparation for COX-1 immunoreactivity, as presented in Fig. 5a. Such an approach normalized these preparation differences in COX-1 expression and yielded approximately 0.9–1.1-fold difference in COX-1 immunoreactivity across each preparation relative to WT. Subsequently, equivalent amounts of immunoreactive COX-1 for each preparation were included in the activity studies.

## COX-1 enzymatic activity

The mean rate of oxygen consumption calculated for the WT COX-1 preparation was 19.7 ± 2.0 μmol/l $O_2$/min/mg microsomal protein. The uninfected negative control demonstrated undetectable oxygen consumption, suggesting detectable oxygen consumption in the COX-1 preparations was due to recombinant COX-1-mediated arachidonic acid metabolism. Pooled analysis of three independent experiments demonstrated the R53H (35.0 ± 4.9%), R78W (36.1 ± 3.9%), K185T (59.2 ± 6.4%), G230S (56.6 ± 3.5%), and L237M (51.0 ± 2.5%) variants had significantly lower metabolic activity relative to WT COX-1 (100.0 ± 7.2%) (Fig. 5b, $P < 0.05$ of each variant versus WT). No significant differences in enzymatic activity were detected in the R8W (103.8 ± 10.0%), P17L (113.3 ± 7.0%), and V481I (121.3 ± 10.2%) variants compared with WT (Fig. 5b). Similar results were obtained in each of the three independent experiments. Moreover, weight-adjusting the calculated oxygen consumption rates according to the mean 0.9–1.1-fold difference in COX-1 immuno-reactivity observed across each normalized preparation did not significantly alter these results (data not shown).

## Inhibition of COX-1 enzymatic activity

The sensitivity of the WT and R8W, P17L, G230S, and L237M variants to inhibition by indomethacin, a non-selective COX inhibitor with greater potency for COX-1 than COX-2 in recombinant systems, was evaluated. The R8W and P17L variants were selected as they are the most frequent nonsynonymous polymorphisms. The G230S and L237M variants were selected on the basis of our basal metabolic activity and modeling results reported above. The effects of increasing indomethacin concentrations on metabolic activity for each preparation relative to vehicle-incubated controls are presented (Fig. 6a-d). From these data, $IC_{50}$ values for each preparation were estimated (Table 4). The P17L and G230S variants demonstrated significantly lower $IC_{50}$ values than those of WT, suggesting presence of these mutations significantly increase COX-1 sensitivity to inhibition by indomethacin. This increase in sensitivity is evident in Fig. 6b and c, respectively. No significant differences in $IC_{50}$ values were observed with the R8W and L237M variants compared with the WT. The R8W variant appeared more resistant to inhibition at lower indo-methacin concentrations relative to WT (Fig. 6a); however, this effect was lost at higher indomethacin concentrations and the estimated $IC_{50}$ value was not statistically different from WT. The L237M variants appeared more sensitive to inhibition at higher indo-methacin concentrations relative to WT (Fig. 6d); however, the estimated $IC_{50}$ value was not statistically different from WT.

To take into account basal COX-1 activity, we compared the rate of oxygen consumption in each preparation after treatment with 25 μmol/l indomethacin relative to WT after treatment with vehicle control (Fig. 6e). The P17L (13.8 ± 1.7%), G230S (4.1 ± 1.3%), and L237M (6.9 ± 2.6%) variants each demonstrated significantly lower metabolic activity compared with WT

(36.7 ± 0.5%) ($P < 0.05$ of each variant versus WT). Significant differences were not observed with the R8W variant (29.4 ± 4.1%) compared with WT. These findings suggest that combination of indomethacin treatment and the P17L, G230S, and L237M variants significantly reduce COX-1 metabolic activity compared with indo-methacin treatment of WT COX-1.

## Discussion

COX-1 and COX-2-derived PGs play a vital role in the regulation of various biological processes in humans, such that nonselective and selective NSAIDs are routinely administered for the prevention and/or treatment of a variety of clinical conditions [1,4-6]. We and others hypothesize that genetic variation in *PTGS1* and *PTGS2* may significantly modify disease risk in humans and/or contribute to interindividual variability in the pharmaco-dynamic response to NSAIDs. Although the functional relevance of genetic variants in *PTGS2* has been evaluated [7,8], functional characterization of human *PTGS1* variants has not been as widely investigated. To guide the design and interpretation of future genetic epidemiology and pharmacogenomic studies, we sought to identify or confirm the existence of genetic polymorphisms in *PTGS1*, characterize the LD structure, and evaluate the functional consequences of selected variants *in vitro*.

We identified multiple variants in both coding and noncoding regions of human *PTGS1* by resequencing 92 healthy individuals. Twenty-four of the 45 variants had been previously reported in the published literature [10-13] and/or publicly available databases (http://www.ncbi.nlm.nih.gov/snp), and were present at comparable frequencies within each ethnic group. Interestingly, seven of the 45 variants were nonsynonymous changes (R8W, R8P, P17L, R78W, K185T, L237M, and V481I), most of which were present at low (≤ 6%) frequencies in distinct ethnic groups. The previously reported R53H and G230S variants [10] were not identified in the egSNP population, but we confirmed their existence at low frequencies in an independent African-American population. Multiple polymorphisms in the *PTGS1* 5′UTR were also identified, including seven (*T-1749C*, *G-1598A*, *A-1202G*, *A-1201G*, *G-1006A*, *A-918G*, and *A-707G*) on the same haplotype in the European/Caucasian and African samples. Moreover, these 5′UTR polymorphisms were also in near-complete LD with the P17L variant in European/Caucasian, but not African individuals. The presence of LD between the *A-707G* and P17L polymorphisms in Caucasians has been previously reported [11,12,14,32]; however, our analysis is the first to suggest that this LD pattern involves six additional polymorphisms further upstream in the 5′UTR. A recent human investigation demonstrated that presence of this variant haplotype was not associated with *PTGS1* RNA expression in oral mucosa [32]. Our preliminary sequence analysis suggests that certain 5′UTR variant alleles may disrupt putative transcription factor binding sites. Further functional characterization of these promoter polymorphisms via transcriptional activation and DNA-binding studies appears necessary.

We expressed recombinant WT COX-1 and the R8W, P17L, R53H, R78W, K185T, G230S, L237M, and V481I mutant proteins and evaluated basal COX-1 metabolic activity *in vitro*. As summarized in Table 5, the R53H, R78W, K185T, G230S, and L237M variants demonstrated significantly lower metabolic activity (35–60%) relative to WT COX-1; although, none completely abolished activity, since as these did not occur at or in immediate proximity to residues critical for substrate binding and/or enzyme activity such as arginine 120 or tyrosine 385 [33-36]. Our protein modeling results suggest the G230S variant may significantly alter COX-1 protein structure. Our interpretation of these structural observations, in conjunction with the observed functional effects, is that the G230S variant disrupts the active conformation of COX-1 by shifting the dimer interface via D228 and W138′. This conformational change could also influence catalysis more directly through an interaction between D228 and R332.

R332 is a member of helix 6 [24], which also includes residues contributing to formation of the active site. A shift in this helix could serve as the mechanism underlying the observed effect on catalytic function.

Similar reductions in enzyme activity were also observed with the R53H, R78W, K185T, and L237M variants, although their predicted impact on COX-1 structure were not as obvious. The L237 residue is conserved across all known COX-1 and COX-2 species, and the L237M variant presumably could influence catalytic activity through its predicted impact on dimerization; however, the association between alterations in COX dimerization and metabolic activity has not been well characterized. The mechanism underlying the alterations in activity observed with the R53H, R78W, and K185T variants does not appear to be explained by our protein modeling results. Recent COX-1 structure–function studies, however, suggest that several amino-acid substitutions with modest influence on arachidonic acid binding to the COX-1 active site can alter the catalytic efficiency and metabolite profile of COX-1-mediated arachidonic acid metabolism [36,37]. Perhaps these variants could reduce overall metabolic efficiency by altering the interaction between arachidonic acid and the active site. Future studies evaluating the mechanism underlying these functional effects appear necessary. No significant changes in enzymatic activity were detected with the R8W, P17L, and V481I variants relative to WT. The R8W and P17L variants occur at amino acids lying within the COX-1 signal peptide sequence, which is posttranslationally cleaved [24,35], and would be unlikely to significantly impact enzymatic activity. Our protein modeling suggests that the V481I variant is also unlikely to significantly alter COX-1 structure or activity. Additional low frequency nonsynonymous variants in *PTGS1* have also been recently discovered (L15-L16del, R108Q, I136V, K341R, R458Q) [10,13,16,38], however, their potential influence on COX-1 metabolic activity has not been investigated. Moreover, the *in vivo* functional consequences of the R53H, R78W, K185T, G230S, L237M, and 5′UTR variants remain to be evaluated via quantification of systemic (plasma, urine) and local (tissue-specific, cell-specific) PG concentrations, particularly as the relative contribution of COX-2 to PG biosynthesis may also be altered in individuals with certain *PTGS1* polymorphisms. *In vitro* and *in vivo* functional studies will substantially aid in the interpretation of genetic epidemiological studies evaluating associations between *PTGS1* polymorphisms and risk of diseases known to involve altered COX-derived PG synthesis, such as cardiovascular and cerebrovascular disease, colorectal cancer, and asthma [4,5].

Inhibition studies with indomethacin demonstrated that the P17L and G230S variants were significantly more sensitive to indomethacin-mediated inhibition of COX-1 activity relative to WT, as determined by estimation of $IC_{50}$ values for each preparation (Table 5). As the P17L variant resides within the COX-1 signal peptide sequence, the mechanism underlying the observed alteration in indomethacin sensitivity is unclear. The estimated $IC_{50}$ values for the R8W and L237M variants were not significantly different from WT; however, COX-1 metabolic activity was significantly lower with the L237M variant relative to WT after inhibition with indomethacin as the L237M variant also had significantly lower basal activity. The estimated indomethacin $IC_{50}$ value for the WT preparation in our study (8.37 μmol/l) was higher than those previously reported with purified COX-1 preparations (approximately 1 μmol/l) [29,30]. This is likely due to our utilization of crude microsomal protein preparations.

Interestingly, a recent human study demonstrated that platelets isolated from Caucasian individuals heterozygous for the P17L variant allele were significantly more sensitive to aspirin-mediated inhibition of $PGF_{2á}$ production compared with WT individuals [12]. Our *in-vitro* data with the P17L variant and indomethacin are consistent with these findings (Table 3), even though aspirin and indomethacin inhibit COX-1 activity via different mechanisms, suggesting individuals carrying this variant may be significantly more sensitive to NSAID-mediated inhibition of COX-1 activity and potentially more susceptible to adverse events such

as gastrointestinal bleeding, renal dysfunction, and/or cardiovascular events [4]. Similar associations may also exist with the G230S and L237M variants; although the population impact of the P17L polymorphism may be more substantial as it is significantly more frequent in both European/Caucasian and African populations. In contrast, human studies have also suggested that the P17L variant may be associated with resistance to aspirin-mediated inhibition of platelet aggregation [14] and aspirin-mediated reduction in risk of colorectal polyps [16]. Importantly, these investigations were also conducted in Caucasian populations, such that presence of the aforementioned *PTGS1* 5′UTR variant alleles, and not the P17L variant allele, may be driving these observed interactions with aspirin therapy. Presence of the P17L variant has also been associated with rofecoxib and celecoxib-mediated inhibition of thromboxane formation *in vivo* [15]. The population evaluated in this investigation consisted of Caucasian, African-American and Asian individuals. As the ethnicities of those carrying the P17L variant allele were not reported, the potential contribution of *PTGS1* 5′UTR polymorphisms could not be ascertained. Collectively, the mechanisms underlying these conflicting *in vitro* and *in vivo* observations remain to be characterized; however, the relative contribution of the P17L and 5′UTR polymorphisms may be an important determinant of NSAID pharmacodynamics in humans. Additional human pharmacogenomic studies evaluating potential associations between *PTGS1* polymorphisms and NSAID pharmacodynamics in both Caucasians and African-Americans, including risk of adverse events, appear warranted.

We acknowledge that certain limitations exist in our analysis. First, utilization of a nonmammalian expression system could significantly impact the expression and function of a recombinant protein, particularly glycosylated proteins such as COX-1. The recombinant COX-1, however, has been expressed in insect-cell systems previously, and has exhibited similar posttranslational processing, glycosylation and activity profiles compared with native COX-1 [29,30]. Second, we recognize the limitations related to evaluation of metabolic activity at a single substrate concentration. The observed differences in the rate of oxygen consumption in certain mutant preparations in comparison with the WT may be a reflection of reduced metabolic capacity (decreased $V_{max}$) and/or reduced substrate binding (increased $K_m$). Evaluation of metabolic activity across a range of substrate concentrations will ultimately be necessary to more completely characterize the enzyme kinetics of each mutant relative to WT. The quantification of oxygen consumption after addition of 100 μmol/l of arachidonic acid, however, has been previously utilized to evaluate COX-1 metabolic activity in recombinant systems [29,30]. Moreover, similar conditions have been employed for $IC_{50}$ determinations of multiple COX inhibitors, including indomethacin [29,30]. We recognize that indomethacin is not utilized clinically as widely as aspirin, or for the same indication, and the clinical applicability of our inhibition studies may not extend to all NSAIDs. Indomethacin, however, has demonstrated greater potency for inhibition of COX-1 than COX-2 and has been widely studied in this recombinant *in vitro* system under these experimental conditions [29,30]. Consequently, we felt it was a more appropriate inhibitor for the initial characterization of selected COX-1 variants.

In summary, the R53H, R78W, K185T, G230S, and L237M variants in *PTGS1* demonstrated significantly lower basal metabolic activity *in vitro* relative to WT COX-1, suggesting individuals carrying these variant alleles may have significantly altered PG biosynthesis *in vivo*. In addition, the P17L and G230S variants were significantly more sensitive to indomethacin-mediated inhibition of COX-1 activity relative to WT, suggesting individuals carrying these variant alleles may be more susceptible to NSAID-associated adverse events. Future studies confirming the *in vivo* relevance of these variants, including their influence on disease susceptibility and NSAID pharmacodynamics, are warranted.

**Acknowledgements**

The authors gratefully acknowledge Dr Joyce Goldstein and Dr Robert Langenbach for their helpful comments during the preparation of this manuscript.

Sponsorship: This publication was made possible by Grant ES012856 to Dr Lee, US Interagency agreement Y1-ES-8054-05, and the Intramural Research Program of the NIH, NIEHS.

## References

1. Smith WL, Garavito RM, DeWitt DL. Prostaglandin endoperoxide H synthases (cyclooxygenases)-1 and -2. J Biol Chem 1996;52:33157–33160. [PubMed: 8969167]
2. Yokoyama C, Tanabe T. Cloning of human gene encoding prostaglandin endoperoxide synthase and primary structure of the enzyme. Biochem Biophys Res Commun 1989;2:888–894.
3. Wang LH, Hajibeigi A, Xu XM, Loose-Mitchell D, Wu KK. Characterization of the promoter of human prostaglandin H synthase-1 gene. Biochem Biophys Res Commun 1993;2:406–411.
4. Warner TD, Mitchell JA. Cyclooxygenases: new forms, new inhibitors, and lessons from the clinic. FASEB J 2004;7:790–804. [PubMed: 15117884]
5. Antman EM, DeMets D, Loscalzo J. Cyclooxygenase inhibition and cardiovascular risk. Circulation 2005;5:759–770.
6. Grosser T, Fries S, Fitzgerald GA. Biological basis for the cardiovascular consequences of COX-2 inhibition: therapeutic challenges and opportunities. J Clin Invest 2006;1:4–15. [PubMed: 16395396]
7. Fritsche E, Baek SJ, King LM, Zeldin DC, Eling TE, Bell DA. Functional characterization of cyclooxygenase-2 polymorphisms. J Pharmacol Exp Ther 2001;2:468–476.
8. Papafili A, Hill MR, Brull DJ, McAnulty RJ, Marshall RP, Humphries SE, et al. Common promoter variant in cyclooxygenase-2 represses gene expression: evidence of role in acute-phase inflammatory response. Arterioscler Thromb Vasc Biol 2002;10:1631–1636.
9. Cipollone F, Toniato E, Martinotti S, Fazia M, Iezzi A, Cuccurullo C, et al. A polymorphism in the cyclooxygenase 2 gene as an inherited protective factor against myocardial infarction and stroke. JAMA 2004;18:2221–2228.
10. Ulrich CM, Bigler J, Sibert J, Greene EA, Sparks R, Carlson CS, et al. Cyclooxygenase 1 (COX1) polymorphisms in African-American and Caucasian populations. Hum Mutat 2002;5:409–410. [PubMed: 12402351]
11. Scott BT, Hasstedt SJ, Bovill EG, Callas PW, Valliere JE, Wang L, et al. Characterization of the human prostaglandin H synthase 1 gene (*PTGS1*): exclusion by genetic linkage analysis as a second modifier gene in familial thrombosis. Blood Coagul Fibrinolysis 2002;6:519–531. [PubMed: 12192304]
12. Halushka MK, Walker LP, Halushka PV. Genetic variation in cyclooxygenase 1: effects on response to aspirin. Clin Pharmacol Ther 2003;1:122–130. [PubMed: 12545150]
13. Hillarp A, Palmqvist B, Lethagen S, Villoutreix BO, Mattiasson I. Mutations within the cyclooxygenase-1 gene in aspirin non-responders with recurrence of stroke. Thromb Res 2003;5–6:275–283.
14. Maree AO, Curtin RJ, Chubb A, Dolan C, Cox D, O'Brien J, et al. Cyclooxygenase-1 haplotype modulates platelet response to aspirin. J Thromb Haemost 2005;10:2340–2345. [PubMed: 16150050]
15. Fries S, Grosser T, Price TS, Lawson JA, Kapoor S, DeMarco S, et al. Marked interindividual variability in the response to selective inhibitors of cyclooxygenase-2. Gastroenterology 2006;1:55–64. [PubMed: 16401468]
16. Ulrich CM, Bigler J, Sparks R, Whitton J, Sibert JG, Goode EL, et al. Polymorphisms in *PTGS1* (= *COX-1*) and risk of colorectal polyps. Cancer Epidemiol Biomarkers Prev 2004;5:889–893. [PubMed: 15159324]
17. Collins FS, Brooks LD, Chakravarti A. A DNA polymorphism discovery resource for research on human genetic variation. Genome Res 1998;12:1229–1231. [PubMed: 9872978]
18. King LM, Ma J, Srettabunjong S, Graves J, Bradbury JA, Li L, et al. Cloning of *CYP2J2* gene and identification of functional polymorphisms. Mol Pharmacol 2002;4:840–852. [PubMed: 11901223]

19. Przybyla-Zawislak BD, Srivastava PK, Vazquez-Matias J, Mohrenweiser HW, Maxwell JE, Hammock BD, et al. Polymorphisms in human soluble epoxide hydrolase. Mol Pharmacol 2003;2:482–490.
20. Bleasby K, Hall LA, Perry JL, Mohrenweiser HW, Pritchard JB. Functional consequences of single nucleotide polymorphisms in the human organic anion transporter hOAT1 (*SLC22A6*). J Pharmacol Exp Ther 2005;2:923–931. [PubMed: 15914676]
21. Barrett JC, Fry B, Maller J, Daly MJ. Haploview: analysis and visualization of LD and haplotype maps. Bioinformatics 2005;2:263–265. [PubMed: 15297300]
22. Knuppel R, Dietze P, Lehnberg W, Frech K, Wingender E. Transfac retrieval program: a network model database of eukaryotic transcription regulating sequences and proteins. J Comput Biol 1994;3:191–198. [PubMed: 8790464]
23. Chenna R, Sugawara H, Koike T, Lopez R, Gibson TJ, Higgins DG, et al. Multiple sequence alignment with the clustal series of programs. Nucleic Acids Res 2003;13:3497–3500. [PubMed: 12824352]
24. Picot D, Loll PJ, Garavito RM. The X-ray crystal structure of the membrane protein prostaglandin H2 synthase-1. Nature 1994;6460:243–249.
25. Kurumbail RG, Stevens AM, Gierse JK, McDonald JJ, Stegeman RA, Pak JY, et al. Structural basis for selective inhibition of cyclooxygenase-2 by anti-inflammatory agents. Nature 1996;6610:644–648. [PubMed: 8967954]
26. Kiefer JR, Pawlitz JL, Moreland KT, Stegeman RA, Hood WF, Gierse JK, et al. Structural insights into the stereochemistry of the cyclooxygenase reaction. Nature 2000;6782:97–101.
27. Davis IW, Murray LW, Richardson JS, Richardson DC. Molprobity: structure validation and all-atom contact analysis for nucleic acids and their complexes. Nucleic Acids Res 2004;(Web Server issue):W615–W619. [PubMed: 15215462]
28. Baek SJ, Wilson LC, Lee CH, Eling TE. Dual function of nonsteroidal anti-inflammatory drugs (NSAIDs): inhibition of cyclooxygenase and induction of NSAID-activated gene. J Pharmacol Exp Ther 2002;3:1126–1131. [PubMed: 12023546]
29. Barnett J, Chow J, Ives D, Chiou M, Mackenzie R, Osen E, et al. Purification, characterization and selective inhibition of human prostaglandin G/H synthase 1 and 2 expressed in the baculovirus system. Biochim Biophys Acta 1994;1:130–139. [PubMed: 7947975]
30. Gierse JK, Hauser SD, Creely DP, Koboldt C, Rangwala SH, Isakson PC, et al. Expression and selective inhibition of the constitutive and inducible forms of human cyclo-oxygenase. Biochem J 1995;305:479–484.
31. Kulmacz, RJ.; Lands, WEM. Cyclo-oxygenase: measurement, purification and properties. In: Denedetto, CC.; McDonald-Gibson, RG.; Nigam, ST.; Slater, F., editors. Prostaglandins and related substances : a practical approach. IRL Press; Washington, District of Columbia: 1987. p. 209-227.
32. Lee YS, Kim H, Wu TX, Wang XM, Dionne RA. Genetically mediated interindividual variation in analgesic responses to cyclooxygenase inhibitory drugs. Clin Pharmacol Ther 2006;5:407–418. [PubMed: 16678543]
33. Shimokawa T, Kulmacz RJ, DeWitt DL, Smith WL. Tyrosine 385 of prostaglandin endoperoxide synthase is required for cyclooxygenase catalysis. J Biol Chem 1990;33:20073–20076.
34. Bhattacharyya DK, Lecomte M, Rieke CJ, Garavito M, Smith WL. Involvement of arginine 120, glutamate 524, and tyrosine 355 in the binding of arachidonate and 2-phenylpropionic acid inhibitors to the cyclooxygenase active site of ovine prostaglandin endoperoxide H synthase-1. J Biol Chem 1996;4:2179–2184. [PubMed: 8567676]
35. Garavito RM, DeWitt DL. The cyclooxygenase isoforms: structural insights into the conversion of arachidonic acid to prostaglandins. Biochim Biophys Acta 1999;2–3:278–287.
36. Thuresson ED, Lakkides KM, Rieke CJ, Sun Y, Wingerd BA, Micielli R, et al. Prostaglandin endoperoxide H synthase-1: the functions of cyclooxygenase active site residues in the binding, positioning, and oxygenation of arachidonic acid. J Biol Chem 2001;13:10347–10357. [PubMed: 11121412]
37. Thuresson ED, Lakkides KM, Smith WL. Different catalytically competent arrangements of arachidonic acid within the cyclooxygenase active site of prostaglandin endoperoxide H synthase-1 lead to the formation of different oxygenated products. J Biol Chem 2000;12:8501–8507. [PubMed: 10722687]

38. Shi J, Misso NL, Duffy DL, Bradley B, Beard R, Thompson PJ, et al. Cyclooxygenase-1 gene polymorphisms in patients with different asthma phenotypes and atopy. Eur Respir J 2005;2:249–256.

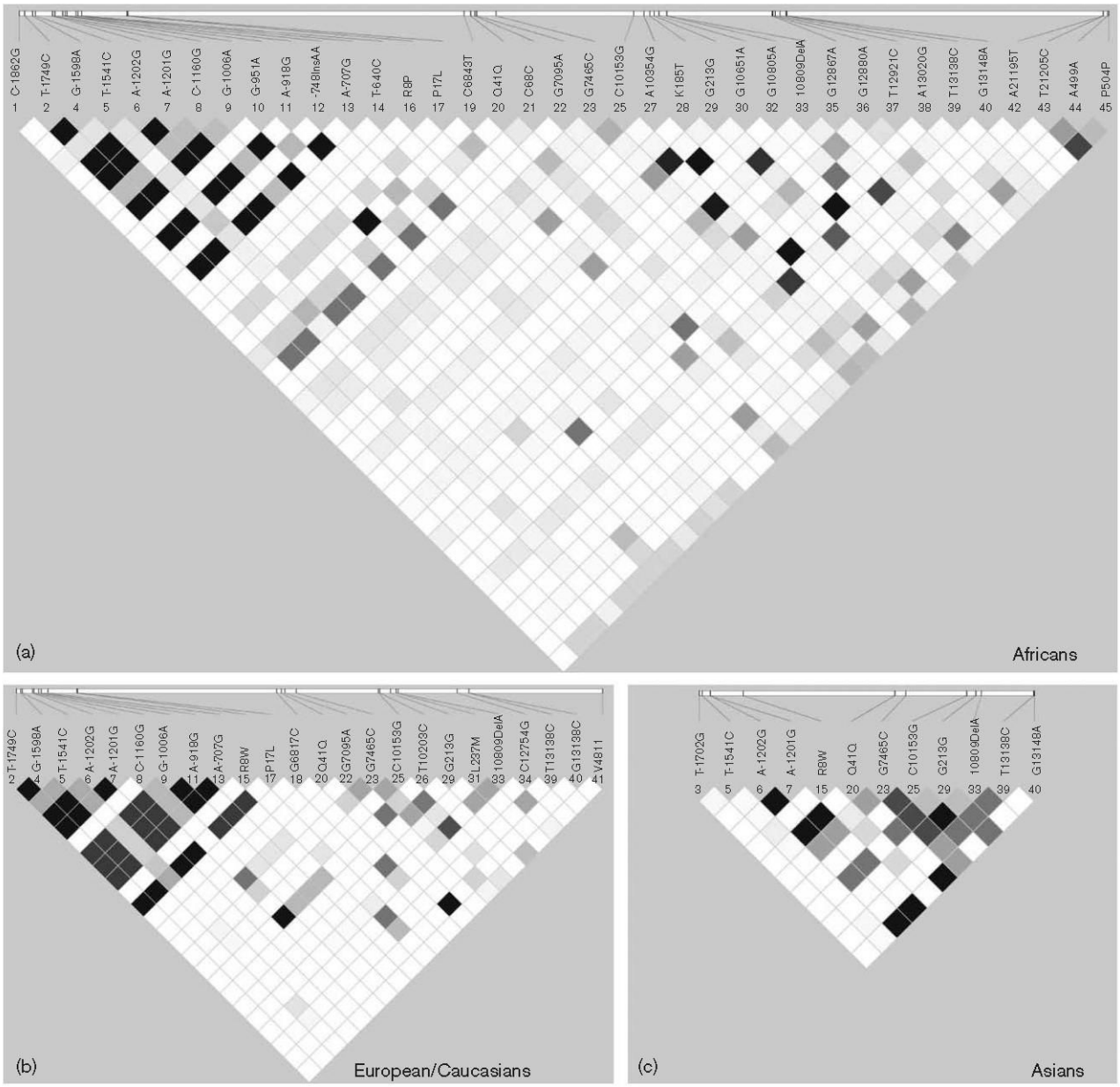


**Fig 1.**

Pairwise estimates of linkage disequilibrium (LD) between each *PTGS1* polymorphism are plotted for the (a) African, (b) European/Caucasian, and (c) Asian ethnic groups using Haploview 3.2. Each polymorphism is numbered according to its position in the *PTGS1* gene as presented in Table 3. Black squares indicate complete LD ($r^2 = 1.0$), white squares indicate zero LD ($r^2 = 0.0$), and increasing intensity of grey indicates increasing degrees of LD.

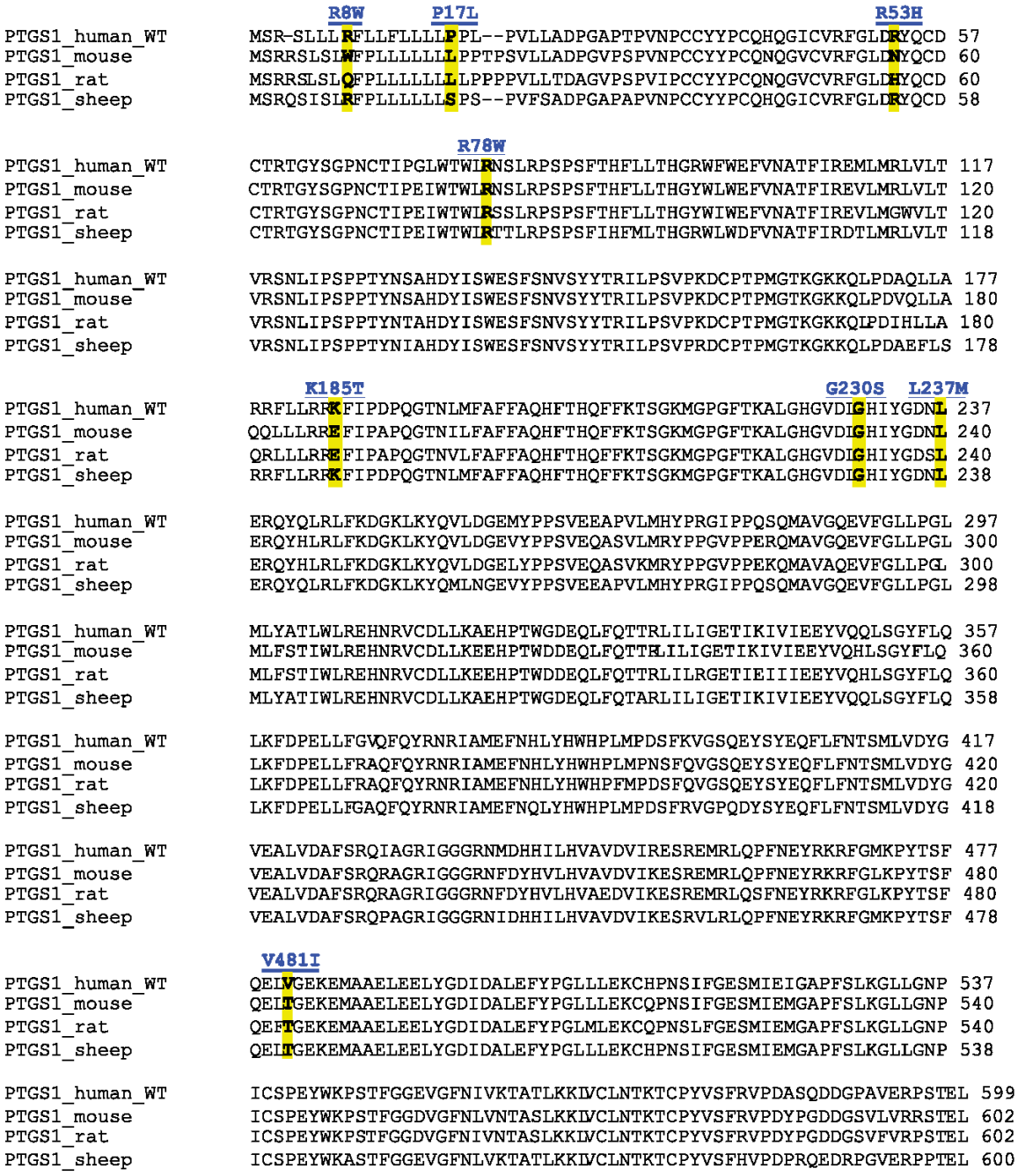


**Fig 2.**

Alignment of the human (Genbank accession number P23219), mouse (AAH05573), rat (NP_058739), and sheep (P05979) COX-1 amino-acid sequences using the ClustalW program. Amino-acid locations of the eight evaluated nonsynonymous variants are highlighted.

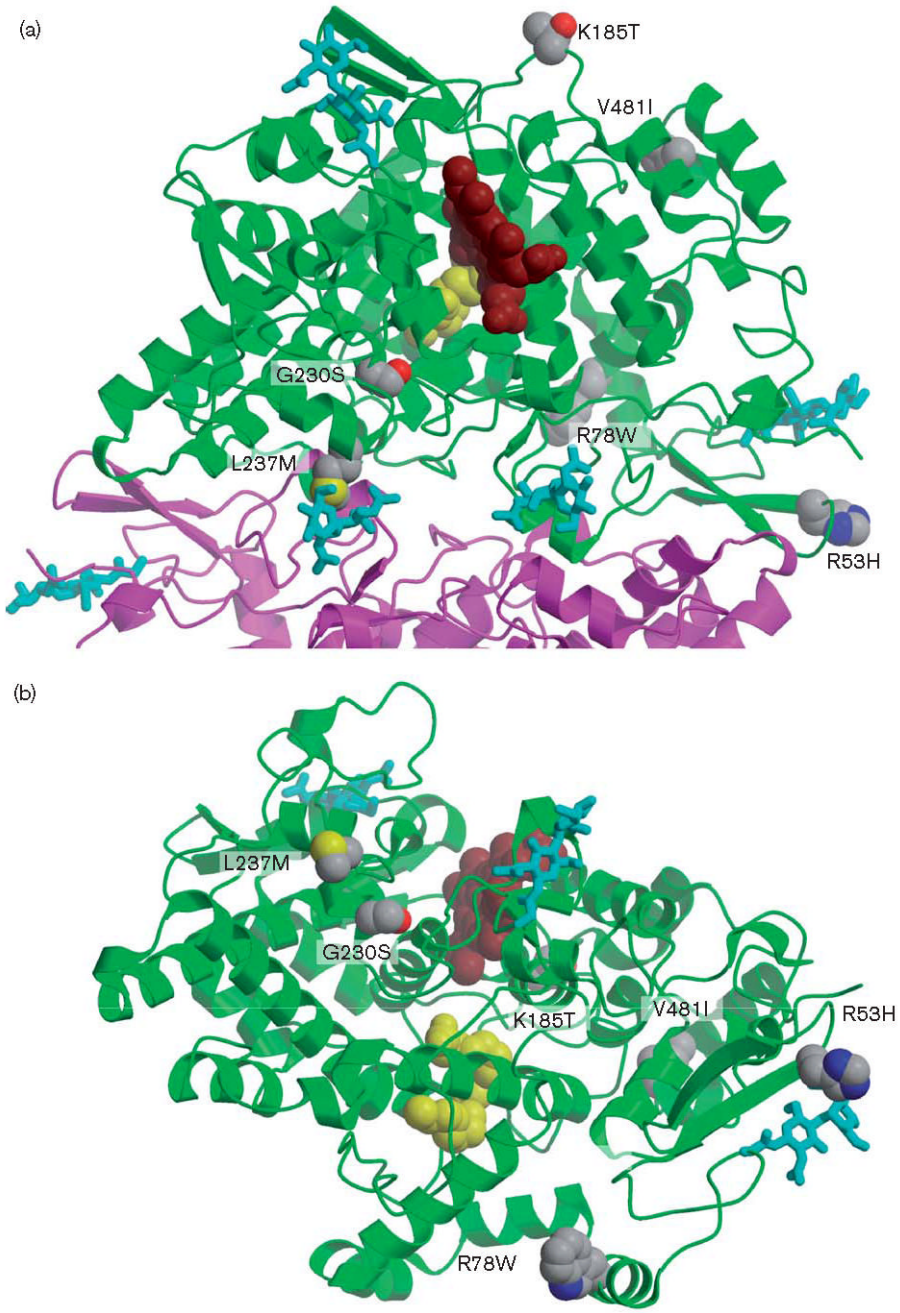


**Fig 3.**

Overview of the COX-1 dimer and the R53H, R78W, K185T, G230S, L237M, and V481I variants, with (a) a top view of the dimer complex and (b) a side view of one monomer facing the dimerization surface. Mutations are illustrated with space-filling atoms. The heme group is shown in maroon, and arachidonic acid is shown in yellow. Sugars are shown in cyan, with two sugars per glycosylation site.

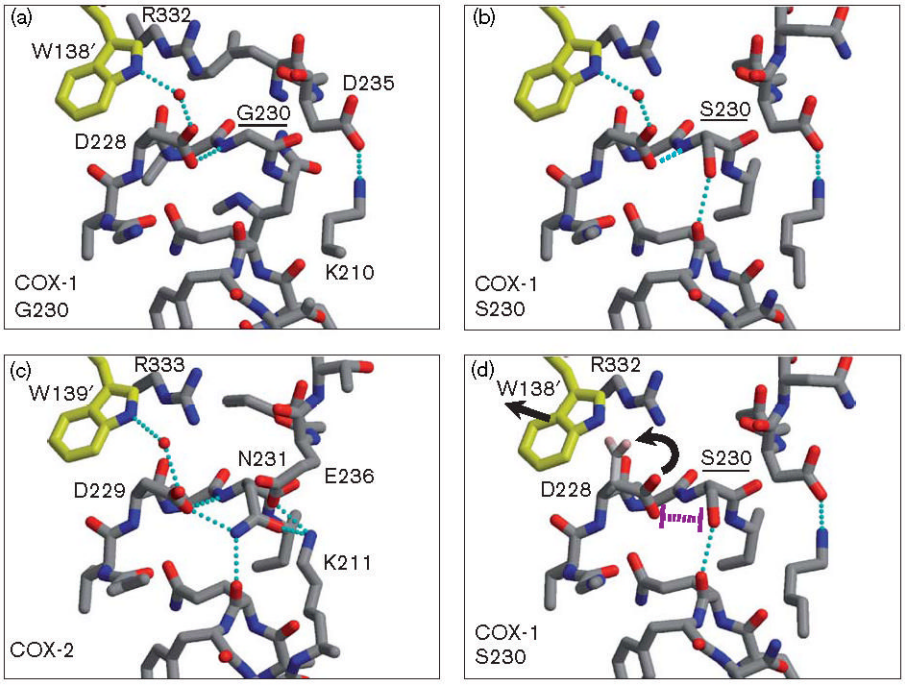


**Fig 4.**

Structural characterization of the G230S variant. (a) The vicinity of G230 in the model of wild-type COX-1. The position of D228 is stabilized by a hydrogen bond to the backbone nitrogen of G230. (b) The G230S substitution allows for only one rotamer position without significant structural changes. (c) The corresponding site in human COX-2 has an N231 in a similar position to the modeled S230 substitution; however, N231 also provides several interactions that help stabilize the observed conformation. (d) In COX-1, S230 destabilizes the observed conformation, which could be avoided by a rotation of D228 towards R332, which also requires a shift in the dimer interaction with W138′.

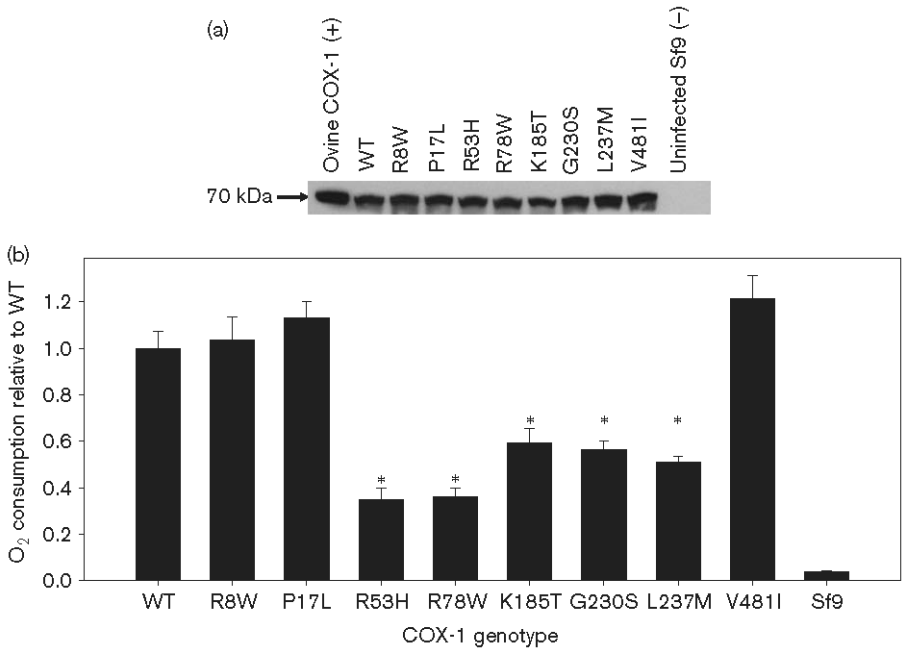


**Fig 5.**

(a) Representative immunoblot of solubilized microsomes containing recombinant wild-type (WT) and eight variant COX-1 proteins. The amount of solubilized microsomal protein loaded per lane for each preparation was normalized to COX-1 immunoreactivity based on previous immunoblots. The WT lane contains 34 μg of microsomal protein. Lane 1 contains COX-1 ovine protein standard (Cayman Chemical, 1 μg) as a positive control. Lane 11 contains solubilized microsomes made from uninfected Sf9 cells (34 μg) as a negative control. (b) Mean ± SEM rate of oxygen consumption for each of the eight variant COX-1 preparations relative to WT. Solubilized microsomal protein from uninfected Sf9 cells were used as a negative control. The data presented are pooled from three independent experiments, each completed in triplicate. The rate of oxygen consumption was significantly associated with the COX-1 microsomal preparation (analysis of variance: $P < 0.001$, $r^2 = 0.78$). *$P < 0.05$ versus WT by a post-hoc Dunnett's test.

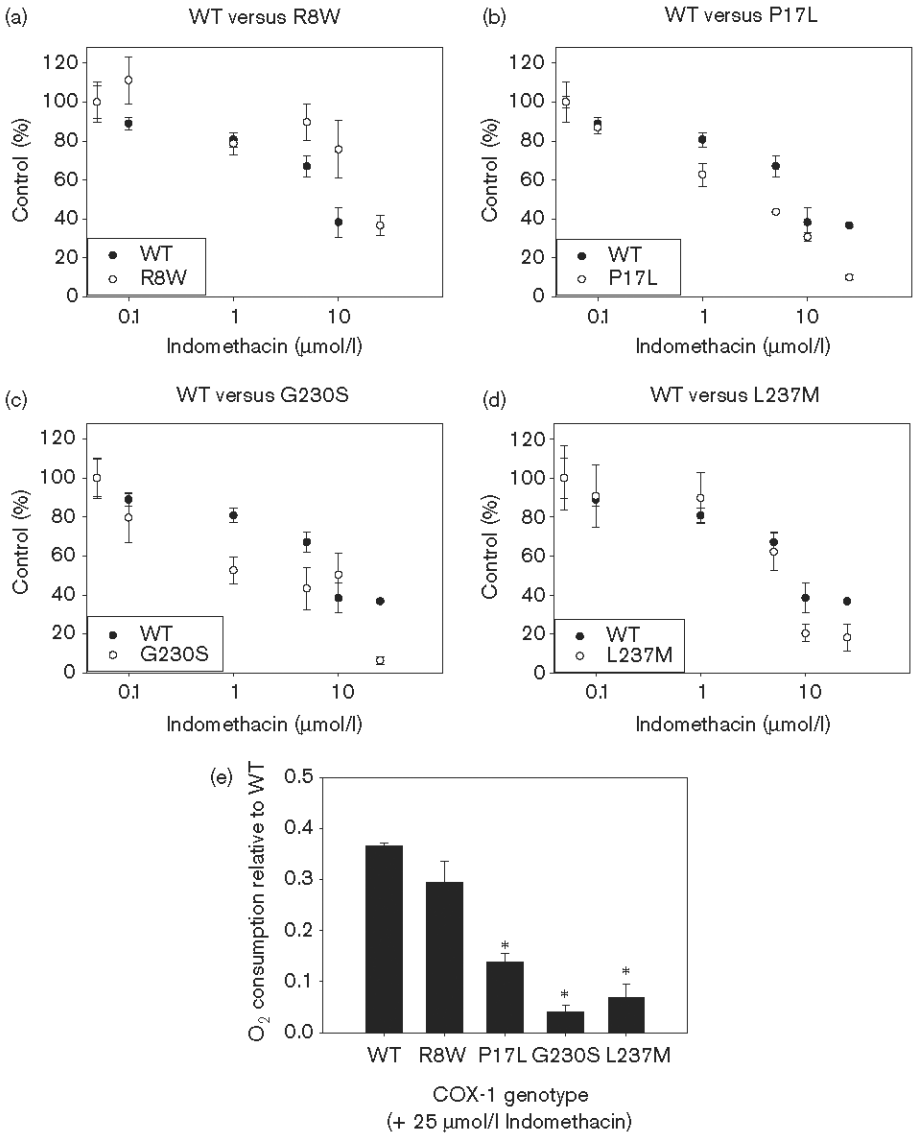


**Fig 6.**

Inhibition of COX-1-mediated arachidonic acid metabolism by increasing concentrations of indomethacin in the (a) R8W, (b) P17L, (c) G230S, and (d) L237M variants compared with wild-type (WT). Values represent the mean ± SEM rate of oxygen consumption calculated at each indomethacin concentration (0.1, 1, 5, 10, and 25 µmol/l) relative to the rate of oxygen consumption detected with vehicle control for each preparation. Each data point includes three independent measurements. (e) Mean ± SEM rate of oxygen consumption for the WT and R8W, P17L, G230S, and L237M variants after incubation with 25 µmol/l indomethacin relative to the rate of oxygen consumption detected after incubation with vehicle control in the WT preparation. Each data point includes three independent measurements. The rate of oxygen consumption after incubation with 25 µmol/l indomethacin was significantly associated with the COX-1 preparation (analysis of variance: $P < 0.001$, $r^2 = 0.93$). *$P < 0.05$ versus WT by a post-hoc Dunnett's test.

**Table 1**

Oligonucleotide primers used for PCR amplification of *PTGS1*

| ***PTGS1* Region** | **Forward primer sequence** | **Reverse primer sequence** |
|---|---|---|
| Promoter 1 | 5′-GAAGGCACAGGGGCTTCCTAGA-3′ | 5′-AGTGGGGAGAAGGTAGATGAGAG-3′ |
| Promoter 2 | 5′-TGTCCTCAGCACCTTTCTTCCCCTA-3′ | 5′-CCCTCCCCCATTCTCACCCAAG-3′ |
| Promoter 3 | 5′-GCATGGGAACACCTTGGGTGAGAATG-3′ | 5′-CAGACTCCACAGCTTACTGGCCGTG-3′ |
| Promoter 4 | 5′-GCCTTCCGATAACTGAGCACCTAC-3′ | 5′-GGCTGCCCGCTTACTTCCTCTGC-3′ |
| Promoter 5 | 5′-CAGGCCAGGCTGGACTGCCCCATTTCT-3′ | 5′-CAGGAGGCCAAGAAAATTCC-3′ |
| Exons 1 and 2 | 5′-CACGCACAGGAGCCTGCACTCTGCGTCC-3′ | 5′-GAAAGGAGGGGGTTGAAACCAGGC-3′ |
| Exon 3 | 5′-CAGGGAGTGAGGGTGGACCAAGAGCG-3′ | 5′-GTCAGGATGGGTGGTTTATGTTCA-3′ |
| Exon 4 | 5′-GTCTCTGTCATGTGTCATTGC-3′ | 5′-GGCACAGAGGGCAGAATACGAGTG-3′ |
| Exon 5 | 5′-GAGCTGGGGGTGGAAACACCCTTGTCA-3′ | 5′-TTCCCAAAGAGAAGAACTGAGCA-3′ |
| Exon 6 | 5′-CTTGACTCAGGGCAAGGGAGTTCAT-3′ | 5′-GGTGCCGGCCCACTGTCGAT-3′ |
| Exon 7 | 5′-GGAAGAAGCAGTTGCCAGATGC-3′ | 5′-CTGTCGCTCCTGGCACAAGCCT-3′ |
| Exon 8 | 5′-GCTGAGGGGAACTGGCAGCTTGGA-3′ | 5′-GCAGGAAGGTAGATACATGCAG-3′ |
| Exon 9 | 5′-CAAGCTGGGCATCTAAATCACTGT-3′ | 5′-GCTGTCGTATGACTGCCATCACT-3′ |
| Exon 10 | 5′-GACTCCCACTGGAAGCTCTTGTC-3′ | 5′-TACACATTGCCGCATGTATTGT-3′ |
| Exon 11 | 5′-CCCAGAAAAAGGTGGACCTGGAA-3′ | 5′-TGGAATGACAAGCACAAAGCTC-3′ |
| Sequence[a] | 5′-GTTTTCCCAGTCACGACG-3′ | 5′-AGGAAACAGCTATGACCAT-3′ |

[a]The 5′ binding site sequence for the forward and reverse energy transfer DNA sequencing primers.

## Table 2

Primers used for the site-directed mutagenesis of human COX-1

| Mutation | Sequences of forward and reverse primers[a] |
|---|---|
| Arg8Trp (R8W) | (F) 5′-CCATGAGCCGGAGTCTCTTGCTC**T**GGTTCTTGCTGTTCCTGCTCC-3′<br>(R) 5′-GGAGCAGGAACAGCAAGAACC**A**GAGCAAGAGACTCCGGCTCATGG-3′ |
| Pro17Leu (P17L) | (F) 5′-GCTGTTCCTGCTCCTGCTCC**T**GCCGCTCCCCGTCCTGCTCG-3′<br>(R) 5′-CGAGCAGGACGGGGAGCGGC**A**GGAGCAGGAGCAGGAACAGC-3′ |
| Arg53His (R53H) | (F) 5′-CCGCTTCGGCCTTGACC**A**CTACCAGTGTGACTGC-3′<br>(R) 5′-GCAGTCACACTGGTAG**T**GGTCAAGGCCGAAGCGG-3′ |
| Arg78Trp (R78W) | (F) 5′-GCCTGTGGACCTGGCTC**T**GGAATTCACTGCGGCCC-3′<br>(R) 5′-GGGCCGCAGTGAATTCC**A**GAGCCAGGTCCACAGGC-3′ |
| Lys185Thr (K185 T) | (F) 5′-GCTTCCTGCTCAGGAGGA**C**GTTCATACCTGACCCCC-3′<br>(R) 5′-GGGGGTCAGGTATGAAC**G**TCCTCCTGAGCAGGAAGC-3′ |
| Gly230Ser (G230S) | (F) 5′-GGGCCATGGGGTAGACCTC**A**GCCACATTTATGGAGAC-3′<br>(R) 5′-GTCTCCATAAATGTGGC**T**GAGGTCTACCCCATGGCCC-3′ |
| Leu237Met (L237M) | (F) 5′-CGGCCACATTTATGGAGACAAT**A**TGGAGCGTCAGTATCAACTGCGGC-3′<br>(R) 5′-GCCGCAGTTGATACTGACGCTCCA**T**ATTGTCTCCATAAATGTGGCCG-3′ |
| Val481Ile (V481I) | (F) 5′-CCTCCTTCCAGGAGCTC**A**TAGGAGAGAAGGAGATGGC-3′<br>(R) 5′-GCCATCTCCTTCTCTCCTA**T**GAGCTCCTGGAAGGAGG-3′ |

[a]Primers were PAGE-purified (Invitrogen). Bold/underlined bases indicate the mutated nucleotides. The R8P mutant was not expressed.

**Table 3**

All variants in *PTGS1* identified from the NIEHS egSNP sequencing project[a]

| Polymorphism | Nucleotide[b] | Location | Amino Acid | Estimated minor allele frequency[c] | | | |
|---|---|---|---|---|---|---|---|
| | | | | Caucasian (*n* = 24) | African (*n* = 24) | Asian (*n* = 24) | All (*n* = 72 or 92[d]) |
| (1) C>G | − 1862 | 5′UTR | - | 0 | 0.02 | 0 | 0.01[d] |
| (2) T>C (rs10306108)[e] | − 1749 | 5′UTR | - | 0.06 | 0.04 | 0 | 0.07[d] |
| (3) T>G | − 1702 | 5′UTR | - | 0 | 0 | 0.02 | 0.01[d] |
| (4) G>A (rs10306109)[e] | − 1598 | 5′UTR | - | 0.06 | 0.04 | 0 | 0.07[d] |
| (5) T>C (rs1330344) | − 1541 | 5′UTR | - | 0.19 | 0.33 | 0.46 | 0.39[d] |
| (6) A>G[e] | − 1202 | 5′UTR | - | 0.06 | 0.04 | 0.02 | 0.07[d] |
| (7) A>G[e] | − 1201 | 5′UTR | - | 0.06 | 0.04 | 0.02 | 0.07[d] |
| (8) C>G | − 1160 | 5′UTR | - | 0.02 | 0.04 | 0 | 0.02[d] |
| (9) G>A[e] | − 1006 | 5′UTR | - | 0.08 | 0.04 | 0 | 0.08[d] |
| (10) G>A | − 951 | 5′UTR | - | 0 | 0.02 | 0 | 0.01 |
| (11) A>G (rs10306110)[e] | − 918 | 5′UTR | - | 0.08 | 0.04 | 0 | 0.04 |
| (12) Insertion AA | − 748 | 5′UTR | - | 0 | 0.08 | 0 | 0.03 |
| (13) A>G (rs10306114)[e] | − 707 | 5′UTR | - | 0.08 | 0.04 | 0 | 0.04 |
| (14) T>C | − 640 | 5′UTR | - | 0 | 0.02 | 0 | 0.01 |
| (15) C>T (rs1236913) | 250 | Exon 2 | R8W | 0.04 | 0 | 0.06 | 0.05[d] |
| (16) G>C | 251 | Exon 2 | R8P | 0 | 0.02 | 0 | 0.01[d] |
| (17) C>T (rs3842787)[f] | 278 | Exon 2 | P17L | 0.06 | 0.06 | 0 | 0.06[d] |
| (18) G>C | 6817 | Intron 2 | - | 0.02 | 0 | 0 | 0.01 |
| (19) C>T | 6843 | Intron 2 | - | 0 | 0.02 | 0 | 0.01 |
| (20) G>A (rs3842788) (NI)[n] G>A | 6975 | Exon 3 | Q41Q | 0.02 | 0.23 | 0.02 | 0.09 |
| (21) C>T (rs10306139) | 7056 | Exon 3 | C68C | 0 | 0.02 | 0 | 0.01 |
| (22) G>A (rs876567) | 7095 | Intron 3 | - | 0.04 | 0.02 | 0 | 0.02 |
| (23) G>C (rs2282169) | 7465 | Intron 3 | - | 0.13 | 0.35 | 0.06 | 0.22[d] |
| (24) C>T | 7501 | Exon 4 | R78W | 0 | 0 | 0 | 0.01[d] |
| (25) C>G (rs10306148) | 10153 | Intron 5 | - | 0.08 | 0.42 | 0.04 | 0.24 |
| (26) T>C | 10203 | Intron 5 | - | 0.02 | 0 | 0 | 0.01 |
| (27) A>G | 10354 | Intron 5 | - | 0 | 0.02 | 0 | 0.01 |
| (28) A>C (rs3842792) | 10476 | Exon 6 | K185T | 0 | 0.04 | 0 | 0.01 |
| (29) C>A (rs5788) | 10561 | Exon 6 | G213G | 0.04 | 0.46 | 0.04 | 0.21 |
| (30) G>A (rs3842794) (NI)[n] G>A | 10651 | Intron 6 | - | 0 | 0.02 | 0 | 0.01 |
| (31) C>A (rs5789) | 10742 | Exon 7 | L237M | 0.04 | 0 | 0 | 0.01 |
| (32) G>A | 10805 | Intron 7 | - | 0 | 0.02 | 0 | 0.01 |
| (33) Deletion A (rs3215925) | 10809 | Intron 7 | - | 0.13 | 0.40 | 0.04 | 0.26 |
| (34) C>G | 12754 | Intron 8 | - | 0.02 | 0 | 0 | 0.01[d] |
| (35) G>A | 12867 | Intron 8 | - | 0 | 0.06 | 0 | 0.02[d] |
| (36) G>A (rs10306153) | 12880 | Intron 8 | - | 0 | 0.31 | 0 | 0.09[d] |
| (37) T>C | 12921 | Intron 8 | - | 0 | 0.04 | 0 | 0.01[d] |
| (38) A>G | 13020 | Intron 8 | - | 0 | 0.02 | 0 | 0.02[d] |
| (39) T>C (rs4836885) | 13138 | Intron 8 | - | 0.04 | 0.41 | 0.02 | 0.23[d] |
| (40) G>A (rs10306230) | 13148 | Intron 8 | - | 0.02 | 0.02 | 0.02 | 0.02[d] |
| (41) G>A (rs5794) | 19389 | Exon 10 | V481I | 0.04 | 0 | 0 | 0.01[d] |
| (42) A>T | 21195 | Intron 10 | - | 0 | 0.04 | 0 | 0.01[d] |
| (43) T>C (rs3842801) | 21205 | Intron 10 | - | 0 | 0.17 | 0 | 0.07[d] |

| Polymorphism | Nucleotide[b] | Location | Amino Acid | Estimated minor allele frequency[c] | | | |
|---|---|---|---|---|---|---|---|
| | | | | Caucasian (*n* = 24) | African (*n* = 24) | Asian (*n* = 24) | All (*n* = 72 or 92[d]) |
| (44) G>A (rs3842802) | 21286 | Exon 11 | A499A | 0 | 0.06 | 0 | 0.02[d] |
| (45) T>C (rs3842803) | 21301 | Exon 11 | P504P | 0 | 0.23 | 0 | 0.08[d] |

5′UTR = 5′ untranslated region.

[a] The R53H and G230S nonsynonymous variants were not identified (NI) in the egSNP population.

[b] Nucleotide position relative to the transcriptional start site (Genbank accession number AF440204).

[c] Number of individuals.

[d] Indicates sequencing data that was obtained in an additional 20 anonymous individuals of unknown ethnicity (*n* = 92 total).

[e] These polymorphisms are in complete or near-complete linkage disequilibrium with one another in both the African ($D'$ = 1.0, $r^2$ = 1.0) and Caucasian ($D'$ = 1.0, $r^2$ = 0.73−1.0) populations. See Fig. 1.

[f] The P17L polymorphism is in complete or near complete linkage disequilibrium with the 5′UTR[e] polymorphisms in the Caucasian population only ($D'$= 1.0, $r^2$ = 0.73−1.0). See Fig. 1.

**Table 4**

Estimated $IC_{50}$ values for indomethacin with WT COX-1 and the R8W, P17L, G230S, and L237M variants

| COX-1 variant | Estimated $IC_{50}$ (μmol/l) (95% confidence interval) |
|---|---|
| WT | 8.37 (5.00−14.0) |
| R8W | 15.3 (11.1−21.0) |
| P17L | 2.80 (1.72−4.56)* |
| G230S | 1.36 (0.54−3.42)* |
| L237M | 3.55 (1.73−7.29) |

WT, wild-type.

* *P*-value < 0.05 versus WT.

**Table 5**

Functional relevance of nonsynonymous polymorphisms in *PTGS1*[a]

| ***PTGS1* variant** | **Amino acid conserved across species**[b] | **Modeling predicted functional impact**[b] | ***In vitro* metabolic activity**[b] | ***In vitro* sensitivity to indomethacin**[b] | ***Ex vivo* sensitivity to aspirin**[c] |
|---|---|---|---|---|---|
| R8W | No | No | ↔ | ↔ | ↔ |
| P17L | No | No | ↔ | ↑ | ↑ or ↓ |
| R53H | No | ?/Yes (minor) | ↓ | ? | ? |
| R78W | Yes | ?/No | ↓ | ? | ? |
| K185T | No | ?/No | ↓ | ? | ? |
| G230S | Yes | Yes (major) | ↓ | ↑ | ? |
| L237M | Yes | Yes (minor) | ↓ | ↔/↑ | ? |
| V481I | No | No | ↔ | ? | ? |

Conflicting results have been reported with the P17L variant, which was in complete linkage disequilibrium with the *A-707G* polymorphism in both populations.

[a] Functional effects indicated as increased (↑), decreased (↓), unchanged (↔), or unknown (?) compared to wild-type.

[b] On the basis of the analyses and *in vitro* functional studies completed in our current investigation.

[c] On the basis of previously published studies by Halushka *et al*. [12] and Maree *et al*. [14] in humans.